Molecular fingerprint of precancerous lesions in breast atypical hyperplasia

Chao Zheng[1],*, Hong Ying Jia[2],*, Li Yuan Liu[1], Qi Wang[3], Hong Chuan Jiang[4], Li Song Teng[5] , Cui Zhi Geng[6], Feng Jin[7], Li Li Tang[8], Jian Guo Zhang[9], Xiang Wang[10], Shu Wang[11], Fernandez-Escobar Alejandro[12], Fei Wang[1], Li Xiang Yu[1], Fei Zhou[1], Yu Juan Xiang[1], Shu Ya Huang[1], Qin Ye Fu[1], Qiang Zhang[1], De Zong Gao[1] , Zhong Bing Ma[1], Liang Li[1], Zhi Min Fan[13] and Zhi Gang Yu[1]

Abstract

Objective: To identify atypical hyperplasia (AH) of the breast by shell-isolated nanoparticle-enhanced Raman spectroscopy (SHINERS), and to explore the molecular fingerprinting characteristics of breast AH.

[1]Department of Breast Surgery, The Second Hospital, Cheeloo College of Medicine, Shandong University, Jinan, Shandong, China
[2]Center of Evidence-based Medicine, The Second Hospital, Cheeloo College of Medicine, Shandong University, Jinan, Shandong, China
[3]Breast Disease Center, Guangdong Maternal and Child Health Care Hospital, Guangzhou, Guangdong, China
[4]Department of General Surgery, Beijing Chaoyang Hospital, Beijing, China
[5]Department of Oncology Surgery, The First Affiliated Hospital of Zhejiang University, Hangzhou, Zhejiang, China
[6]Breast Center, the Fourth Hospital of Hebei Medical University, Shijiazhuang, Hebei, China
[7]Department of Breast Surgery, the First Affiliated Hospital of China Medical University, Shenyang, Liaoning, China
[8]Department of Breast Surgery, Xiangya Hospital of Central South University, Changsha, Hunan, China

[9]Department of General Surgery, the Second Affiliated Hospital of Harbin Medical University, Harbin, Heilongjiang, China
[10]Department of Breast Surgery, Cancer Hospital, Chinese Academy of Medical Sciences, Beijing, China
[11]Breast Disease Center, Peking University People's Hospital, Beijing, China
[12]Translational Research Program, University of Toronto, Toronto, Ontario, Canada
[13]Department of Breast Surgery, the First Hospital of Jilin University, Changchun, Jilin, China

*These authors contributed equally to this work.

Corresponding author:
Zhi Gang Yu, Department of Breast Surgery, The Second Hospital, Cheeloo College of Medicine, Shandong University, Jinan, Shandong 250033, China.
Email: yzg@medmail.com.cn

Methods: Breast hyperplasia was studied in 11 hospitals across China from January 2015 to December 2016. All patients completed questionnaires on women's health. The differences between patients with and without breast AH were compared. AH breast lesions were detected by Raman spectroscopy followed by the SHINERS technique.

Results: There were no significant differences in clinical features and risk-related factors between patients with breast AH (n = 37) and the control group (n = 2576). Fifteen cases of breast AH lesions were detected by Raman spectroscopy. The main different Raman peaks in patients with AH appeared at 880, 1001, 1086, 1156, 1260, and 1610 cm^{-1}, attributed to the different vibrational modes of nucleic acids, β-carotene, and proteins. Shell-isolated nanoparticles had different enhancement effects on the nucleic acid, protein, and lipid components in AH.

Conclusion: Raman spectroscopy can detect characteristic molecular changes in breast AH lesions, and may thus be useful for the non-invasive early diagnosis and for investigating the mechanism of tumorigenesis in patients with breast AH.

Introduction

Although the incidence of breast diseases continues to increase steadily, improvements in breast cancer diagnosis and health awareness campaigns have facilitated the early diagnosis of breast cancer and pre-cancerous lesions.[1,2] However, current efforts to prevent the malignant transformation of early-stage disease have been limited.[3] Clinicians should therefore not only diagnose high-risk lesions accurately, but should also carry out appropriate investigations and interventions to reduce the risk and incidence of invasive carcinoma at the individual and population levels. The breast cancer progression model introduced by Wellings and Jensen[4] initially suggested that normal cells in the terminal ductal lobular unit first progress to atypical hyperplasia (AH), then develop into ductal carcinoma in situ, and finally to invasive carcinoma. Preventing the malignant transformation of breast AH cells could significantly decrease the occurrence of cancer,[2,5] and understanding the pathologic stage of AH is thus extremely important in terms of the clinical diagnosis.

Raman spectroscopy is a complementary, safe, noninvasive, and nonradiative vibrational spectroscopic method that can be used to continuously monitor soft tissues with high resolution, without pretreatment, and which can provide valuable information on samples through molecular fingerprinting.[6–8] Different molecules have different vibrational modes, resulting in a unique molecular fingerprint that can be used to identify breast AH.[9] However, despite its high specificity in terms of molecular features, the use of Raman spectroscopy is limited by poor efficiency in the inelastic scattering processes and the consequently relatively weak signal.[10] To overcome this drawback, Li et al. proposed $Au@SiO_2$ shell-isolated

nanoparticle-enhanced Raman spectroscopy (SHINERS),[11] in which the Au core generates surface-enhanced Raman spectroscopy, and the shell is used to protect the Au core from degradation using precisely fabricated nanostructures. This technique has greater versatility, allowing it to be applied in surface and spectroscopic sciences, for drug and food safety inspection, and in other applications from the semiconductor industry to living cells.[12]

In this study, we identified patients with breast hyperplasia from 11 hospitals. We collected basic patient information and clinical, imaging, and breast pathology data. Clinical features and risk-related factors were compared between patients with and without AH. In addition, AH was detected by Raman spectroscopy and SHINERS and its clinical features and molecular fingerprinting characteristics were analyzed, to investigate the potential molecular mechanisms of transformation from normal breast tissue to AH or cancer, and to explore the potential roles of these techniques in the prevention and treatment of breast diseases, and in reducing the risk of breast cancer.

Materials and methods

Study population

We identified outpatients with breast hyperplasia from the following 11 hospitals between January 2015 and December 2016: The Second Hospital of Shandong University, The First Hospital of Jilin University, The First Affiliated Hospital of China Medical University, The Second Affiliated Hospital of Harbin Medical University, Peking University People's Hospital, Cancer Hospital Chinese Academy of Medical Sciences, Beijing Chao Yang Hospital, The Fourth Hospital of Hebei Medical University, Xiangya Hospital of Central South University, The First Affiliated Hospital of Zhejiang University, and Guangdong Maternal and Child Health Care Hospital.

Patients were included in the study if they met the following criteria: breast pain and/or breast lumps in line with a clinical diagnosis of breast hyperplasia; aged 25 to 75 years; and breast ultrasound and mammography (above 35 years old) showed no signs of malignancy. The nature of the breast pain varied, and could be bilateral or unilateral. Most patients referred to the pain as a tingling sensation, typically associated with the menstrual cycle. Breast lumps were usually detected as palpable areas of mammary tissue thickening or abnormal masses with an irregular shape, unclear boundaries, and firm or soft to touch. Patients with mammary gland hyperplasia were divided into three clinical types according to the clinical manifestations: "pain type", "mass type", and "mixed type".

Patients were prevented from participating in the study if they met any of the following exclusion criteria: past medical history of benign breast tumors; long-term use of oral contraceptives; breast-feeding or pregnant; breast ultrasound and mammography showed signs of malignancy; refusal to participate; and aged <25 years or >75 years. We performed a sample-size calculation. Based on a comprehensive analysis with an expected non-remission rate of breast hyperplasia of 15% and a loss to follow-up rate of 20% (upper limit), we determined that the study should initially include about 5000 patients.

Data collection

Questionnaire surveys were conducted by face-to-face interviews, and each study group was assigned a unique questionnaire code. The questionnaire included the following information: demographic characteristics, lifestyle habits, self-assessment

scale (fatigue scale-14, irritability, depression, and anxiety self-rating scale), breast clinical examination data, imaging data, breast ultrasound and mammography data, and breast pathology data (on the premise of informed consent, patients with pain to palpation (>4 points for pain score), palpable mass, or patients who strongly required breast biopsy to confirm the pathological diagnosis). All participants were informed of the purpose and methods of the study and provided signed informed consent. All personal information remained confidential. This study was approved by the Ethics Committee of the Second Hospital of Shandong University (Number: 20140307, date of approval: August 19, 2014). All patients underwent core needle biopsy (Bard Biopsy Systems, Franklin Lakes, NJ, USA; type: MC1616, gauge size: 16 g, length of sample notch: 1.9 cm). After the operation, the samples were frozen immediately at -20 to $-25°C$ and two contiguous sections (6 μm thick) were cut from each sample using a freezing microtome (CM3050S, Leica, Germany). One section was stained with hematoxylin and eosin for routine histopathological analysis by three experienced breast pathologists; the other section was transported to a research laboratory in liquid nitrogen. The histopathology of the sampled region of the tissue was defined as the maximum grade for the sample.

Raman spectroscopy

The histopathological sections from the breast AH lesions were sent to the State Key Laboratory of Supramolecular Structure and Materials, Jilin University, for Raman spectroscopy detection using a confocal Raman system (LabRAM ARAMIS, Horiba Jobin Yvon, Edison, NJ, USA) with a spatial resolution of 3 λ, power 5 mW, and using a 633-nm HeNe laser as the excitation source. The system's focusing objective was a 50× microscope, the spot size of the laser focused on the tissue was 2 μm, the spectral scanning range was 700 to 2000 cm^{-1}, and a 4-notch filter (HORIBA Jobin Yvon, Edison, NJ, USA) was used to filter the strong Rayleigh-scattered lights. The spectral scanning parameters were set as follows: integration time of 60 s and three accumulations. The Raman shift axis was calibrated using characteristic vibration bands recorded from a silicon wafer. The settings were kept constant for all the spectral measurements. All spectral parameter settings and spectral data processing methods have been described in detail in previous studies.[13] After obtaining spontaneous Raman spectra, Au@SiO2 shell-isolated nanoparticles (SHINs) were added to the surface of the sections to collect SHINERS spectra. We used SHINs with an average Au core diameter of 55 nm covered by 2-nm ultrathin silica shells. Before collecting the spectra, 10 μL of 100 nM concentrated SHINs solution was added uniformly to each tissue section.

Statistical analyses

The database was created using Epidata 3.1 software (Epidata Association, Odense, Denmark). Data were entered twice by different people, and the Epidata software could be used to perform automatic logic checks to conduct the data review. All data were analyzed using SPSS Statistics for Windows, version 21.0 (SPSS Inc., Chicago, IL, USA). In the description of each indicator, continuous variables were presented as mean ± standard deviation and categorical variables as ratio or composition ratio. Continuous variables were compared between groups using t-tests and categorical variables using χ^2 tests. A two sided P-value < 0.05 was considered to be statistically significant.

Ethics

All procedures performed involving human participants were in accordance with the ethical standards of the Second Hospital of Shandong University Research Committee. Written informed consent was obtained from all participants by investigators as part of the interview.

Results

Clinical characteristics of breast AH

A total of 3516 patients were enrolled in the study, of whom 2613 (76.31%) received a pathological diagnosis based on voluntary biopsy. All patients were aged 25 to 75 years (mean age 41.75±9.12 years). Thirty-seven patients (1.42%; mean age 43.75± 9.42 years) were diagnosed with breast AH. Clinical features were compared between the 37 patients with AH (case group, n = 37) and the rest of the patients (control group, n = 2576). Age of menarche was similar in the AH and control groups (14.39±1.94 years and 14.07±1.67 years, respectively). Significantly more patients with AH lived in urban areas ($P = 0.028$), had hypertension ($P = 0.001$), and were smokers ($P = 0.034$). There were no significant differences in any other factors, including age at first childbirth and body mass index (Table 1).

There was no significant difference in clinical type between patients with AH and the control group, and no significant differences in breast ultrasound findings, including mammary duct dilatation, breast echo inhomogeneity, breast mass ratio, and blood flow signals. However, patients with AH showed significantly more irregularly shaped masses on breast ultrasound ($P < 0.001$). There were no significant differences in the proportion of dense-type breast and breast masses, calcification of the mass, and structural distortion on breast mammography, but AH was significantly more likely to be characterized by irregular ($P < 0.001$) and unclear boundaries ($P < 0.001$).

SHINERS examination of breast AH

The molecular characteristics of AH lesions were initially examined by Raman spectroscopy, and SHINs were then added to the surface of the sections for SHINERS. Fifteen cases of breast AH lesions were detected, including 167 Raman spectra and 188 SHINERS spectra. We also examined Raman spectra for 10 normal breast (NB) tissues, including 110 Raman spectra and 132 SHINERS spectra for comparison. Figure 1 shows the mean Raman and SHINERS spectra for breast AH and normal tissues. Raman spectra variations within AH and NB breast tissues for three randomly selected AH and NB individual spectra without SHINs are shown in the Appendix.

The characteristic peaks in the NB tissues appeared at 1088, 1156, 1260, 1302, 1440, 1660, and 1740 cm^{-1}, and the main characteristic Raman peaks were classified as lipid and protein peaks, including amide III, amino acid residues, and collagen (Figure 1).[14,15] The Raman lipid peaks in AH tissues appeared at 1120, 1300, 1440, and 1742 cm^{-1}, and the main lipid characteristic peaks were shifted by 2 to 3 cm^{-1}. In addition to the strong characteristic lipid peaks, there were relatively inconspicuous characteristic peaks at 854, 1030, 1156, 1261, 1575, and 1660 cm^{-1}, which could be attributed to the vibrational modes of C-H, α-helices, and amino acid residues in proteins. The characteristic band assignments of AH are shown in Table 2.[14,15] After the addition of SHINs, some characteristic peaks were shifted by 2 to 3 cm^{-1}, the relative intensities of 1088 and 1156 cm^{-1} were significantly increased, and 1494 cm^{-1} appeared. These three

Table 1. Basic clinical characteristics in patients with breast atypical hyperplasia.

Variable	Case n (%)	Control n (%)	χ^2	P
Type	36 (100)	2438 (100)	1.636	0.651
Pain	13 (36.11)	963 (39.50)		
Mass	13 (36.11)	654 (26.83)		
Mixed	10 (27.78)	821 (33.67)		
Location	37 (100)	2443 (100)	4.839	0.028
Urban	27 (72.97)	1340 (54.85)		
Rural	10 (27.03)	1103 (45.15)		
Number of births	36 (100)	2520 (100)	0.265	0.876
0	3 (8.33)	190 (7.54)		
1–2	32 (88.89)	2217 (87.98)		
≥3	1 (2.78)	113 (4.48)		
Menopause	36 (100)	2473 (100)	0.157	0.692
Yes	3 (8.33)	165 (6.67)		
No	33 (91.67)	2308 (93.33)		
Menstrual pattern	30 (100)	2317 (100)	0.765	0.382
Regular	25 (83.33)	2050 (88.48)		
Irregular	5 (16.67)	267 (11.52)		
Breastfeeding	34 (100)	2322 (100)	0.998	0.318
Yes	29 (85.29)	2099 (90.40)		
No	5 (14.71)	223 (9.60)		
Breast pain	37 (100)	2528 (100)	1.698	0.193
Yes	8 (21.62)	800 (31.65)		
No	29 (78.38)	1728 (68.35)		
BMI	37 (100)	2530 (100)	0.513	0.474
<24	24 (64.86)	1726 (68.22)		
≥24	13 (35.13)	804 (31.77)		
Diabetes mellitus	36 (100)	2558 (100)	0.367	0.545
Yes	1 (2.78)	39 (1.52)		
No	35 (97.22)	2519 (98.48)		
Hypertension	37 (100)	2561 (100)	10.971	0.001
Yes	6 (16.22)	117 (4.57)		
No	31 (83.78)	2444 (95.43)		
Family history of breast cancer	37 (100)	2567 (100)	0.527	0.468
Yes	1 (2.70)	139 (5.41)		
No	36 (97.30)	2428 (94.59)		
Cigarette smoking	37 (100)	2570 (100)	4.518	0.034
Yes	5 (13.51)	140 (5.45)		
No	32 (86.49)	2430 (94.55)		
Alcohol drinking	37 (100)	2566 (100)	1.535	0.215
Yes	13 (35.14)	670 (26.11)		
No	24 (64.86)	1896 (73.89)		
Physical activity	37 (100)	2566 (100)	2.981	0.084
Yes	31 (83.78)	1817 (70.81)		
No	6 (16.22)	749 (29.19)		
Sleep satisfaction	36 (100)	2483 (100)	0.200	0.655
Satisfied	28 (77.78)	1850 (74.51)		
Dissatisfied	8 (22.22)	633 (25.49)		
Life satisfaction	36 (100)	2512 (100)	1.901	0.168
Satisfied	31 (86.11)	2229 (88.73)		
Dissatisfied	5 (13.88)	283 (11.27)		

BMI, body mass index.
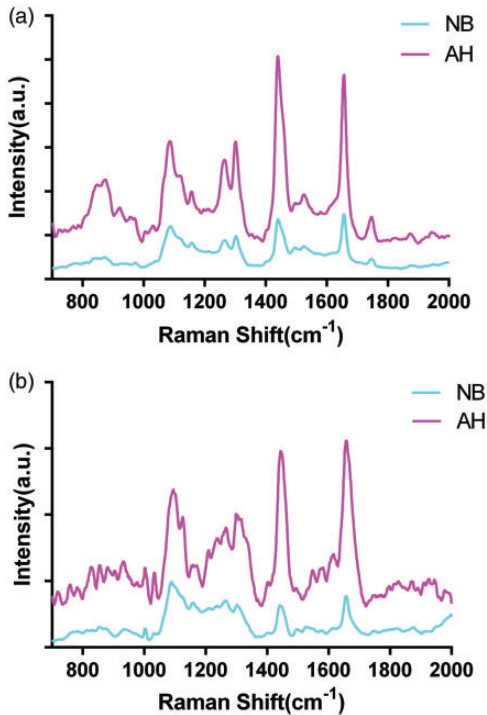
Figure 1. Mean Raman spectra and shell-isolated nanoparticle-enhanced Raman spectroscopy (SHINERS) spectra of atypical hyperplasia and normal breast tissues. (a) SHINERS spectra; (b) Raman spectra. AH, atypical hyperplasia; NB, normal breast; a.u., arbitrary unit.

characteristic peaks were assigned to different vibrational modes of the O-P-O stretch in lipids, nucleic acids, and β-carotene.

The difference spectra between AH and NB breast tissues was calculated by subtracting the mean NB spectrum from the AH spectrum (Figure 2). The most obvious positive characteristic peaks appeared at 720, 880, 1001, 1300, 1422, and 1660 cm^{-1}, which were attributed mainly to the characteristic peaks of proteins and nucleic acids. In contrast, there was an apparent negative peak at 1156 cm^{-1}, corresponding to the characteristic carotenoid peak. We calculated the differences in relative contents of nucleic acids, proteins, and lipids

for the peaks between AH and NB (Figure 3), and showed that 880 and 970 cm^{-1} were characteristic nucleic acid peaks, 1260 and 1440 cm^{-1} were attributed to lipids, and 1610 and 1660 cm^{-1} belonged to proteins. There were significant differences in the six characteristic peaks between the two tissues ($P < 0.001$).

To discriminate between AH and NB tissues, we used SHINs to enhance the main chemical components (proteins, nucleic acids, and lipids) and compared the results with the unenhanced spectral peaks (Figure 4). Comparing the characteristic peak enhancements of the three main components, the characteristic protein peak at 1001 cm^{-1}, which belongs to the symmetry ring stretching vibration of phenylalanine, showed a weakening effect, and the AH lesions had a more pronounced performance. In contrast, the amide I band and α-helix at 1660 cm^{-1} showed strong enhancement. Further analysis showed that, in the characteristic lipid peaks, the 1260 cm^{-1} characteristic $=$C–H peak had the worst enhancement effect in AH and NB, and enhancement was most obvious in the C$=$O stretching vibration of 1742 cm^{-1}. SHINs had similar peak-enhancing effects on nucleic acids in these two tissues.

Discussion

The occurrence and progression of breast cancer is generally believed to be a continuous process from normal epithelium to hyperplasia, AH, carcinoma in situ, and finally to invasive carcinoma.[1,16] AH is a major precancerous lesion,[17] and early treatment and monitoring during this important pathological stage can have significant impacts on the incidence of breast cancer.[5] However, the current large-scale epidemiological investigation showed that breast AH cannot be diagnosed and monitored accurately based on clinical features and risk factors.

Table 2. Peak assignments of Raman spectra of breast tissue

NB	AH	Peak assignment
720	720	C–C twisting mode of tyrosine
781	784	C–N (membrane phospholipid head)/adenine
830	828	U,C,T ring breathing, DNA
854	854	Out of plane ring breathing tyrosine/O-P-O stretch DNA
880	880	DNA
931	928	C–C stretch of proline ring/glucose/lactic acid
935		C–C stretch of proline ring and valine and protein backbone (a-helix conformation)/glycogen
1001	1001	symmetric ring breathing mode of phenylalanine
1031	1030	C–H in plane bending mode of phenylalanine
1088	1086	C–C stretch, O–P–O stretch (nucleic acids)
1118	1120	V (C–C) of lipids from trans-segments
1156	1156	β-carotene
1210	1211	Tryptophan and phenylalanine V mode
1260	1261	(Amide III) C–N stretching mode of protein
1302	1300	CH_2 deformation (lipid)/adenine, cytosine
1440	1440	CH_2 deformation (lipid)
1527	1527	C=C stretching mode of β-carotene
1573	1575	Tryptophan, nucleic acid s(guanine, adenine) TRP protein
	1610	(Amide I, α-helix),V (C=O) of proteins collagen, elastin
1660	1660	C=O stretching mode of phospholipids
1740	1742	Tryptophan and phenylalanine V mode

AH, breast atypical hyperplasia; NB, normal breast tissues.

AH is characterized by filling and distention of the involved ducts by monotonous epithelial cells forming architecturally complex patterns, including cribriform-like secondary lumens or micropapillary formations.[3] This histological feature provides the basis for the using molecular fingerprinting Raman spectroscopy for the early detection and diagnosis of AH lesions of the breast. Raman spectroscopy is a non-invasive and informative spectroscopic technique widely used for the early diagnosis of cancer.[18,19] It can directly detect tumor tissue samples and quickly determine the internal molecular structure and characteristics of the samples, with the ability to identify subtle molecular changes in biological components even at the initial stage of the lesions.[20] Our team has performed Raman spectroscopy to detect breast cancer microcalcification, thus confirming its diagnostic utility.[13,21,22]

Compared with normal tissues, the C-O bond stretching vibration of the β-sheet of amide I band (1610 cm^{-1}) in protein appeared in breast AH tissues, indicating that the C-O group in the protein was severely damaged when the breast epithelial cells became cancerous, resulting in destruction of the protein conformation space.[23] Importantly, 1088 cm^{-1} in the characteristic nucleic acid peak represents the phosphoric acid skeleton stretching vibration mode of the DNA. During breast epithelium carcinogenesis, single and double strand DNA breaks occur, resulting in a spectral shift and decreased intensity.[14] This peak shifts to 1086 cm^{-1} in AH and also in breast invasive carcinoma, indicating that the partial DNA double strands have already begun to break in AH. This finding
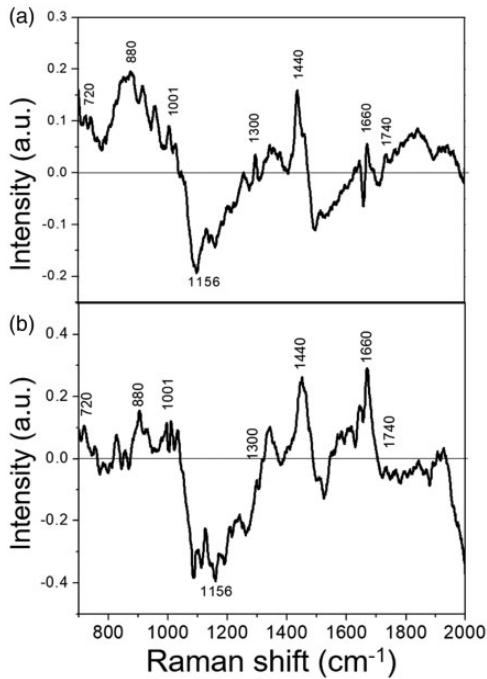
Figure 2. Difference spectra obtained by subtracting mean normal breast from atypical hyperplasia spectrum. (a) Shell-isolated nanoparticle-enhanced Raman spectroscopy spectra; (b) Raman spectra. NB, normal breast; AH, atypical hyperplasia, a.u., arbitrary unit.

Figure 3. Differences in relative contents of nucleic acids, proteins, and lipids between atypical hyperplasia (AH) and normal breast (NB) tissues. Characteristic nucleic acid peaks were 880 and 970 cm^{-1}, lipid peaks were 1260 and 1440 cm^{-1}, and protein peaks were 1610 and 1660 cm^{-1}. The differences in all six peaks between the AH and NB tissues were significant ($P < 0.001$). NB, normal breast tissue; AH, breast atypical hyperplasia, a.u., arbitrary unit.
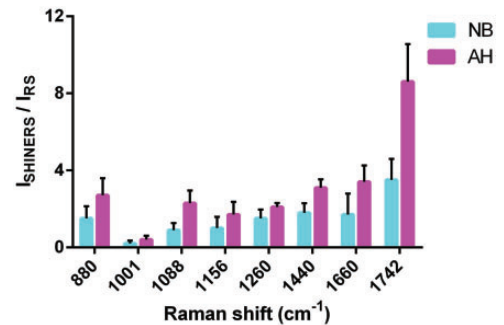
Figure 4. The ratios of shell-isolated nanoparticle-enhanced Raman spectroscopy and Raman intensities of characteristic peaks of the main components in normal breast and atypical hyperplasia tissues. The characteristic protein peaks were 1001 and 1660 cm^{-1}, lipids were 1260, 1440, and 1742 cm^{-1}, nucleic acids were 880 and 1088 cm^{-1}, and 1156 cm^{-1} was attributed to β-carotene. $P < 0.001$ for 1088, 1660, and 1742 cm^{-1} and $P = 0.001$ for 880 cm^{-1}. In addition, the enhancement ratio differences for 1156 and 1440 cm^{-1} were significantly different ($P = 0.037$), but the differences for the 1001 and 1260 cm^{-1} groups were not significant. NB, normal breast tissues; AH, breast atypical hyperplasia, SHINERS, shell-isolated nanoparticle-enhanced Raman spectroscopy; RS, Raman scattering.

further confirms the progression model of breast cancer.

We calculated the difference spectra by subtracting the mean NB spectrum from the breast AH spectrum. The more obvious positive characteristic peaks were attributed to proteins and nucleic acids, and the apparent negative peak at 1156 cm^{-1} belonged to β-carotene. These results are in agreement with previous findings by Chowdary et al.[6] and coincided with the proliferation of tumors.[24,25] In addition, there were significant differences in the relative contents of nucleic acids, proteins, and lipids between AH and NB. The current results support earlier investigations by other laboratories in terms of Raman

spectra for normal tissues being dominated by lipids, but the negative results for β-carotene may be related to free radical oxidation of pigments.[23] According to Shafer-Pelitier et al.,[26] carotenoids show no or minor specificity and cannot be treated as a marker for discrimination of normal, benign, and malignant breast tissues.

To further pinpoint the molecular features of breast AH, we investigated the specific enhancements of the principal chemical constituents of each tissue, including nucleic acids, lipids, and proteins, by SHINERS. The SHINs showed different enhancements in the characteristic peaks in AH and NB. The characteristic protein peak at 1001 cm^{-1}, which belongs to the symmetry ring stretching of phenylalanine, showed a weakening effect, and the atrophic effect of AH was more obvious. Phenylalanine has been considered to be an indicator of uncontrolled cell proliferation,[27] and is widely present in the formation of collagen fibrils in tumors during cancer development and proliferation.[28] The different enhancement effects demonstrated here thus need further study. In contrast, the characteristic protein peak at 1660 cm^{-1} (amide I band, α-helix) showed approximately 8-fold enhancement. Further analysis of the characteristic lipid peaks revealed that the peak of $C=O$ stretching vibration at around 1742 cm^{-1} had the greatest enhancement (about 3.5-fold), while the $=CH$ vibration plane at 1260 cm^{-1} had the worst enhancement (about 1.5-fold).

Li et al. and Anema et al.[11,29] found that the vibration mode parallel to the surface of the substrate was less effective, while the vibration mode perpendicular to the substrate surface was significantly enhanced. Liang et al. and Wen et al.[13,30] suggested that $=CH$ plane vibration may be adsorbed on the surface of the nanoparticles in parallel to the shell, while the $C=O$ stretching vibration of lipids is vertically adsorbed on the surface of the shell to block the nanoparticles, resulting in different degrees of enhancement. The current study found that the SHINs produced the greatest enhancement of the characteristic peak in both tissues, and the $C=O$ stretching vibration lipid peak at around 1742 cm^{-1} was most enhanced in AH and NB. The peak enhancement factor in NB tissue was 8.6-fold, but this peak was only increased 3.5-fold in AH lesions of the breast. It is therefore possible to distinguish between these two tissues based on the difference in the enhancement factor.

This study explored the clinical features and risk-related factors in patients with AH, as well as their molecular fingerprinting characteristics. However, this study had some inherent limitations. Notably, this was a descriptive, case control study based on retrospective data, leading to recall bias. Furthermore, no follow-up data were obtained because the follow-up time was not long enough. The Raman spectral features were not analyzed by mathematical methods, and future studies should therefore be conducted using mathematical models to identify AH lesions and NB, to fully exploit the spectral data. Notwithstanding its limitations, the results of this large population-based study may clarify the characteristic molecular changes occurring in breast AH lesions, and may provide a reference and basis for future research.

Conclusion

We used Raman spectroscopy to explore the differences and relationships between breast AH and NB tissues at the molecular level. We discovered that some single and double DNA strands have started to break in AH, while β-carotene is decreased, the spatial protein conformation is disrupted, and amino acid residues are increased.

Raman spectroscopy can thus identify breast AH, and may provide a method for its non-invasive early diagnosis as well as for the study of cancer mechanisms, thus compensating for the current lack of diagnosis and monitoring methods for AH in the clinical setting.

Data availability

The datasets generated and analyzed during the current study are available from the corresponding author on reasonable request.

Declaration of conflicting interest

The authors declare that there is no conflict of interest.

ORCID iDs

Li Song Teng https://orcid.org/0000-0001-6470-9017
De Zong Gao https://orcid.org/0000-0003-1644-3626
Zhi Gang Yu https://orcid.org/0000-0002-3093-4491

References

1. Danforth DN. Molecular profile of atypical hyperplasia of the breast. *Breast Cancer Res Treat* 2018; 167: 9–29.
2. Kader T, Hill P, Rakha EA, et al. Atypical ductal hyperplasia: update on diagnosis, management, and molecular landscape. *Breast Cancer Res* 2018; 20: 39.
3. Hartmann LC, Degnim AC, Santen RJ, et al. Atypical hyperplasia of the breast–risk assessment and management options. *N Engl J Med* 2015; 372: 78–89.
4. Wellings SR and Jensen HM. On the origin and progression of ductal carcinoma in the human breast. *J Natl Cancer Inst* 1973; 50: 1111–1118.
5. Murray M. Pathologic high-risk lesions, diagnosis and management. *Clin Obstet Gynecol* 2016; 59: 727–732.
6. Krishna CM, Kurien J, Mathew S, et al. Raman spectroscopy of breast tissues. *Expert Rev Mol Diagn* 2008; 8: 149–166.
7. Kallaway C, Almond LM, Barr H, et al. Advances in the clinical application of Raman spectroscopy for cancer diagnostics. *Photodiagnosis Photodyn Ther* 2013; 10: 207–219.
8. Zhang C, Winnard PT Jr, Dasari S, et al. Label-free Raman spectroscopy provides early determination and precise localization of breast cancer-colonized bone alterations. *Chem Sci* 2018; 9: 743–753.
9. Huh YS, Chung AJ and Erickson D. Surface enhanced Raman spectroscopy and its application to molecular and cellular analysis. *Microfluid Nanofluidics* 2009; 6: 285.
10. Zheng C, Shao W, Paidi SK, et al. Pursuing shell-isolated nanoparticle-enhanced Raman spectroscopy (SHINERS) for concomitant detection of breast lesions and microcalcifications. *Nanoscale* 2015; 7: 16960–16968.

11. Li JF, Huang YF, Ding Y, et al. Shell-isolated nanoparticle-enhanced Raman spectroscopy. *Nature* 2010; 464: 392–395.

12. Li JF, Tian XD, Li SB, et al. Surface analysis using shell-isolated nanoparticle-enhanced Raman spectroscopy. *Nat Protoc* 2012; 8: 52.

13. Liang L, Zheng C, Zhang H, et al. Exploring type II microcalcifications in benign and premalignant breast lesions by shell-isolated nanoparticle-enhanced Raman spectroscopy (SHINERS). *Spectrochim Acta A Mol Biomol Spectrosc* 2014; 132: 397–402.

14. Kast RE, Serhatkulu GK, Cao A, et al. Raman spectroscopy can differentiate malignant tumors from normal breast tissue and detect early neoplastic changes in a mouse model. *Biopolymers* 2008; 89: 235–241.

15. Stone N, Kendall C, Smith J, et al. Raman spectroscopy for identification of epithelial cancers. *Faraday Discuss* 2004; 126: 141–157; discussion 69-83.

16. Bombonati A and Sgroi DC. The molecular pathology of breast cancer progression. *J Pathol* 2011; 223: 307–317.

17. Hamdy SM, Latif AK, Drees EA, et al. Prevention of rat breast cancer by genistin and selenium. *Toxicol Ind Health* 2012; 28: 746–757.

18. Santos IP, Barroso EM, Bakker Schut TC, et al. Raman spectroscopy for cancer detection and cancer surgery guidance: translation to the clinics. *Analyst* 2017; 142: 3025–3047.

19. Darrigues E, Nima ZA, Majeed W, et al. Raman spectroscopy using plasmonic and carbon-based nanoparticles for cancer detection, diagnosis, and treatment guidance. Part 1: diagnosis. *Drug Metab Rev* 2017; 49: 212–252.

20. Wan QS, Wang T and Zhang KH. Biomedical optical spectroscopy for the early diagnosis of gastrointestinal neoplasms. *Tumour Biol* 2017; 39: 1010428317717984.

21. Hu C, Wang J, Zheng C, et al. Raman spectra exploring breast tissues: comparison of principal component analysis and support vector machine-recursive feature elimination. *Med Phys* 2013; 40: 063501.

22. Paidi SK, Rizwan A, Zheng C, et al. Label-free Raman spectroscopy detects stromal adaptations in premetastatic lungs primed by breast cancer. *Cancer Res* 2017; 77: 247–256.

23. Abramczyk H, Placek I, Brozek-Pluska B, et al. Human breast tissue cancer diagnosis by Raman spectroscopy. *Spectroscopy* 2008; 22: 113–121.

24. Barman I, Dingari NC, Saha A, et al. Application of Raman spectroscopy to identify microcalcifications and underlying breast lesions at stereotactic core needle biopsy. *Cancer Res* 2013; 73: 3206–3215.

25. Haka AS, Shafer-Peltier KE, Fitzmaurice M, et al. Diagnosing breast cancer by using Raman spectroscopy. *Proc Natl Acad Sci U S A* 2005; 102: 12371–12376.

26. Shafer-Peltier KE, Haka AS, Fitzmaurice M, et al. Raman microspectroscopic model of human breast tissue: implications for breast cancer diagnosis in vivo. *J Raman Spectrosc* 2002; 33: 552–563.

27. Moreno M, Raniero L, Arisawa EÂL, et al. Raman spectroscopy study of breast disease. *Theor Chem Acc* 2010; 125: 329–334.

28. Rehman S, Movasaghi Z, Tucker AT, et al. Raman spectroscopic analysis of breast cancer tissues: identifying differences between normal, invasive ductal carcinoma and ductal carcinoma in situ of the breast tissue. *J Raman Spectrosc.* 2007; 38: 1345–1351.

29. Anema JR, Li JF, Yang ZL, et al. Shell-isolated nanoparticle-enhanced Raman spectroscopy: expanding the versatility of surface-enhanced Raman scattering. *Annu Rev Anal Chem (Palo Alto Calif)* 2011; 4: 129–150.

30. Wen BY, Jin X, Li Y, et al. Shell-isolated nanoparticle-enhanced Raman spectroscopy study of the adsorption behaviour of DNA bases on Au(111) electrode surfaces. *Analyst* 2016; 141: 3731–3736.

Appendix
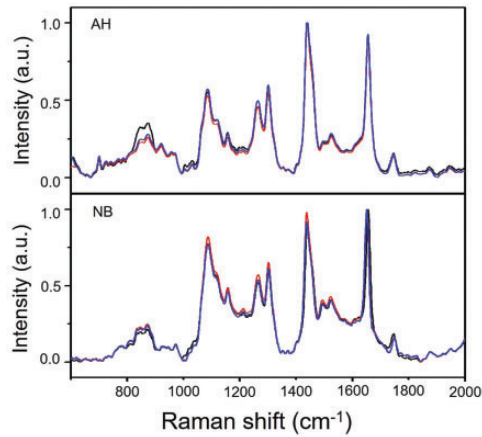
Figure 5. Raman spectra variations in atypical hyperplasia (AH) and normal breast (NB) tissues. Three individual AH and NB spectra without Au@SiO$_2$ shell-isolated nanoparticles were randomly selected from different patients. The variations in Raman spectrum characteristics between different patients were minimal. a.u., arbitrary unit.